$Tl^+Tl^0(1)$-like dimer centers in KCl and RbCl doped with Tl^+, In^+, and Ga^+: A resonant Raman study

Hilde Fleurent * and Dirk Schoemaker
Department of Physics, University of Antwerp (Universitaire Instelling Antwerpen), B-2610 Wilrijk (Antwerp), Belgium

Wim Joosen
Foundation for Fundamental Research on Matter (FOM), Institute for Atomic and Molecular Physics, 1098 SJ Amsterdam, The Netherlands
(Received 20 November 1989)

The Raman spectra of x-ray-irradiated KCl and RbCl, doped with Ga^+ and In^+ impurities, demonstrate the presence of $Ga^+Ga^0(1)$ and $In^+In^0(1)$ dimer centers through a completely polarized defect-induced broadband spectrum, similar to the one reported for $Tl^+Tl^0(1)$ in these alkali halides under resonant excitation of its third optical transition (OT3) [W. Joosen *et al.*, Phys. Rev. B **32**, 6748 (1985)]. The dynamical modes of this broadband spectrum are shown to possess $C_{4v}:A_1$ character, consistent with a high degree of σ polarization of the OT3 of the dimer center. The broadband spectrum is characteristic for the host crystal and shows the same polarization properties and spectral composition as the monomer $M^0(1)$ center (M=Tl,In,Ga). This observation supports the model, derived from optically detected magnetic resonance experiments, of a Tl dimer, in which the unpaired electron is moving between two perturbed $Tl^0(1)$-like configurations. The absence of low-frequency vibrational modes in the dimer spectra is probably related to this nonadiabatic electron motion. Despite the resonant enhancement and the different defect structure, the $M^+M^0(1)$, broadband spectrum in KCl and RbCl exhibits common features with the Tl^+-induced first-order Raman spectrum [R. T. Harley *et al.*, Phys. Rev. B **3**, 1365 (1971)], indicating a larger electron density in the anion vacancy for the third excited state than for the ground state.

I. INTRODUCTION

A specific topic in color centers studies of the last decade has certainly been the investigation of heavy-metal impurity defects in alkali halides and their potential laser activity. The most prominent of these, the $Tl^0(1)$ defect, is produced after x-ray irradiation in Tl^+-doped KCl and was identified by electron paramagnetic resonance (EPR) and optical absorption as a substitutional Tl atom perturbed by an adjacent anion vacancy[1,2] (Fig. 1). An accurate determination of the absorption bands was obtained by tagged absorption experiments,[3] by tagged magnetic circular dichroism (MCD),[4] and by optically detected magnetic resonance (ODMR),[4] establishing the first three optical transitions (called OT1, OT2, OT3 in this paper) in KCl to peak at 1060, 725, and 550 nm, respectively. The model of a neutral Tl atom perturbed by an axial crystal field was appropriate in describing the three lowest optical transitions.[3] The laser-active properties of the $Tl^0(1)$ defect in KCl and KBr (Refs. 5 and 6) stimulated further EPR measurements in Tl^+-doped RbCl, KBr,[7] and NaCl,[8] and led also to the study of the isoelectronic $In^0(1)$ and $Ga^0(1)$ defects in KCl,[2,9] for which ODMR experiments identified their OT3 at 610 and 605 nm, respectively.[10,11] The absence of any significant emission of the latter two defects eliminated them as potential laser defect candidates.

The ODMR experiments on $Tl^0(1)$ in KCl (Ref. 4) also revealed a thallium dimer center, the Tl^+-perturbed $Tl^0(1)$ [denoted $Tl^+Tl^0(1)$], which consists of two adjacent Tl^+ ions around one anion vacancy, sharing one unpaired electron[12] (Fig. 1). The orientation of the nearly axial hyperfine tensor **A** is mainly determined by the anion vacancy, as is the case for the $Tl^0(1)$ defect,[1] while the **g**-tensor values are substantially different for both centers, revealing $C_{4v}\langle 100\rangle$ symmetry for $Tl^0(1)$ and $C_{2v}\langle 110\rangle$ for $Tl^+Tl^0(1)$. The optical-absorption and emission properties of the $Tl^+Tl^0(1)$ center are also very similar to those of the $Tl^0(1)$ defect. Therefore it was suggested that the unpaired electron, which is mainly in a $6p_z$ orbital

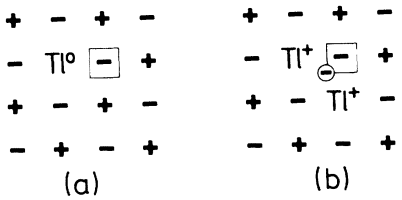

FIG. 1. Schematic representation in a {100} plane of the structure of the $Tl^0(1)$ (a) and $Tl^+Tl^0(1)$ (b) defects in alkali halides. The $Tl^0(1)$ consists of a neutral Tl atom and a nearest-neighbor anion vacancy. The $Tl^+Tl^0(1)$ involves two adjacent Tl^+ ions around one anion vacancy, sharing one unpaired electron. The electron is hopping between the two, slightly perturbed $Tl^0(1)$-like configurations (see text).

along the line connecting the Tl^+ ion and the anion vacancy, is hopping (or tunneling) between two $Tl^0(1)$-like configurations. Motional averaging yields the experimental EPR hyperfine interaction parameters and the g-tensor components. The overlap of the Tl^0 6*p*-electron wave function with the 6*s* function of the second Tl^+ ion is reflected in a tilting of the 6*p* orbital with respect to the [100] axis of 12.1° in KCl and 13.6° in RbCl. In the optical data there is no motional averaging, as is shown by the strong similarity with the properties of the $Tl^0(1)$ transitions. These observations are directly connected with the jump (or tunneling) frequency of the unpaired electron, which is fast compared to the ODMR microwave frequency, and slow compared to the optical frequencies. The above model[12] is denoted as "hopping model" throughout this paper.

The presence of an absorption band in the visible region makes the Tl monomer[13] and dimer centers[14] accessible for resonant Raman measurements in their OT3. In both cases a completely polarized defect-induced spectrum is detected, onto which for $Tl^0(1)$ a low-frequency mode is superimposed, originating from the vibrational motion of the Tl nucleus along the fourfold axis. The broadband Raman spectra of the $Ga^0(1)$ and $In^0(1)$ defects in KCl (Ref. 15) show an analogous spectral composition. The low-frequency mode is shifted to higher frequencies, due to the smaller mass of these two ions.

In this paper resonant Raman measurements are reported for x-ray-irradiated KCl and RbCl, containing Ga^+ and In^+ impurities. In Sec. III we focus on the identification of the $Ga^+Ga^0(1)$ and $In^+In^0(1)$ defects using their production procedures, optical-absorption data, and specific features of the Raman spectra. The polarization properties and the spectral composition of the dimer spectra are discussed in Sec. IV. The behavior-type analysis[16] of the Raman spectrum and the close resemblance of the $M^0(1)$ and $M^+M^0(1)$ spectra are in agreement with the hopping model.[12] The spectral composition of the dimer spectra is compared with the Tl^+-induced first-order spectrum[17] and evidence for the *F*-center character of the third excited (Σ) state of the $M^0(1)$-like defects is presented.

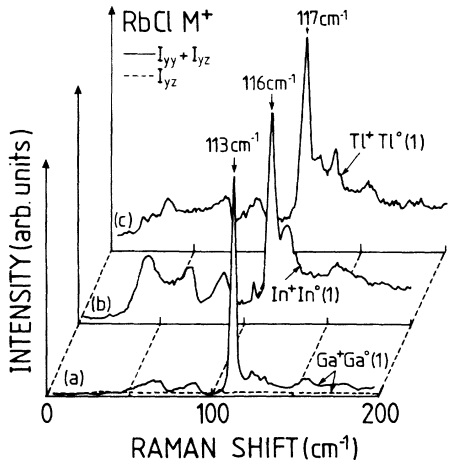

FIG. 3. Resonant Raman spectra of the $M^+M^0(1)$ dimer (M=Tl, In, Ga) in (a) RbCl:Ga^+ (676.4 nm, 30 mW), (b) RbCl:In^+ (647.1 nm, 30 mW), and (c) RbCl:Tl^+ (647.1 nm, 30 mW). The 43-cm^{-1} mode does not belong to $In^+In^0(1)$. Sample treatment: (a) 20 min x ray at 295 K, 10 min *F* bleach at 295 K, (b) and (c) 30 min x ray at 295 K, 1 min *F* bleach at 295 K.

II. EXPERIMENTAL DETAILS

Most of the samples were cut from boules with about 1 mol % of GaCl (InCl) in the melt. The Raman spectra

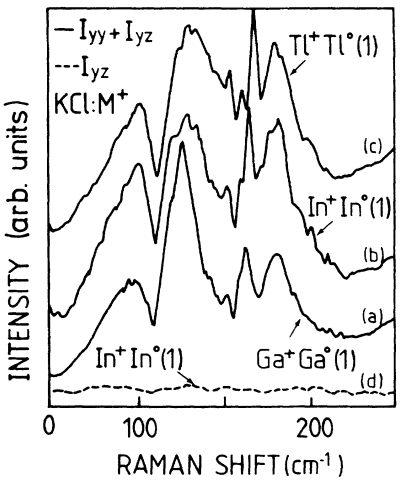

FIG. 2. Resonant Raman spectra of the $M^+M^0(1)$ dimer (M=Tl, In, Ga) in (a) KCl:Ga^+ (647.1 nm, 30 mW), (b) KCl:In^+ (676.4 nm, 55 mW), and (c) KCl:Tl^+ (647.1 nm, 30 mW). Sample treatment: (a) 20 min x ray at 295 K, 10 min *F* bleach at 250 K, 15 min OT3 bleach at 300 K, (b) 40 min x ray at 295 K, 15 min *F* bleach, and (c) 1 h x ray at 295 K, 5 min *F* bleach at 250 K.

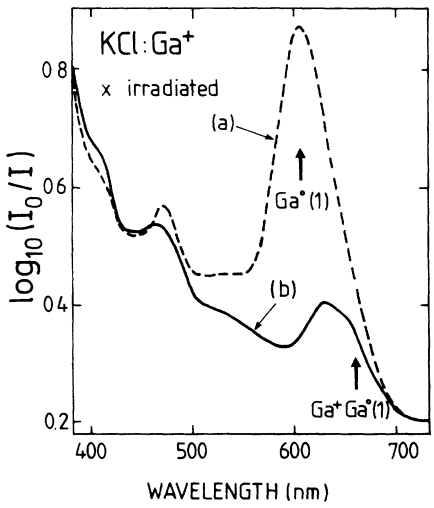

FIG. 4. Absorption spectra of KCl:Ga^+ (a) after 20 min x-ray irradiation at RT with a subsequent 30 min bleach at 474 nm and (b) after a subsequent $Ga^0(1)$ OT3 bleach at 618 nm at RT.

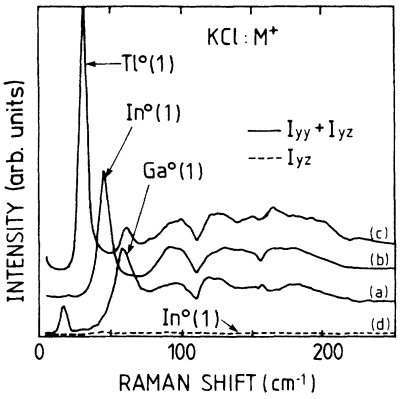

FIG. 5. Resonant Raman spectra of the $M^0(1)$ defect (M=Tl, In, Ga) in (a) KCl:Ga^+ (647.1 nm, 145 mW), (b) KCl:In^+ (647.1 nm, 145 mW), and (c) KCl:Tl^+ (514.5 nm, 30 mW). The excitation wavelengths and laser power of these spectra are indicated. Sample treatment: (a) 20 min x ray at RT, 10 min F bleach at 250 K, (b) 20 min x ray at RT, 15 min F bleach at 266 K, and (c) 1 h x ray at RT, 5 min F bleach at 250 K.

were excited between 10 and 15 K with the 676.4-, 647.1-, 568.2-, and 530.9-nm lines of the Kr^+ laser and the 632.8-nm line of the He-Ne laser. Parallel Raman and optical-absorption measurements were performed. A halogen lamp and a suitable interference filter were used for the optical bleachings of F and $M^0(1)$ centers.

III. IDENTIFICATION OF THE $M^+M^0(1)$ SPECTRA

The identification of the $Ga^+Ga^0(1)$ and $In^+In^0(1)$ dimer centers is based on the similarity in the production procedures and on the interpretation of the resonant Raman spectra and optical-absorption data. The Raman spectra of the $M^+M^0(1)$ defects under OT3 excitation are presented in Figs. 2 and 3. Optical-absorption data for x-ray-irradiated KCl:Ga^+ are shown in Fig. 4. For clarity, the OT3 Raman spectra of $Tl^0(1)$, $In^0(1)$, and $Ga^0(1)$ in KCl (Ref. 15) are also shown in Fig. 5.

A. Production procedures

1. *X-ray irradiation and pulse-anneal experiments*

The production properties of the Ga^+- and In^+-doped KCl samples were investigated by parallel Raman scattering and optical-absorption measurements. X-ray irradiation at 77 K produces the F band (i.e., the $1s$-$2p$ electronic transition of the F center) at about 540 nm in optical absorption. The Raman spectra under 676.4-nm excitation show the broadband Raman spectrum, previously reported by Pan and Lüty.[18] A pulse anneal to temperatures above 220 K (the onset temperature for anion vacancy mobility in KCl) yields the formation of (a) the monomer $In^0(1)$ and $Ga^0(1)$ defects, as shown by the presence of the optical-absorption band at 610 and 605 nm, respectively,[10] and the low-frequency Raman mode at 43 and 59 cm^{-1}, respectively, under 647.1 nm excitation[15] (Fig. 5), and (b) the dimers $In^+In^0(1)$ and $Ga^+Ga^0(1)$, as confirmed by the detection of the dimer spectra of Fig. 2 under 676.4-nm excitation. This will be discussed further in Sec. III B. This treatment establishes the participation of mobile anion vacancies in the defect formation. After x-ray irradiation at temperatures higher than 240 K the dimer Raman spectra are produced immediately.

2. *Various optical bleachings*

The dimer center concentration can be enhanced by suitable optical treatments. An F bleach at 533 nm ($T > 220$ K) promotes both the $M^0(1)$ and $M^+M^0(1)$ production in KCl. Optical excitation at room temperature (RT) in the absorption band of the $Ga^0(1)$ and $In^0(1)$ defect leads to a complete disappearance of the OT3 absorption bands and the low-frequency Raman modes [Fig. 2(a)]. This so-called OT3 bleach considerably enhances the intensity of the dimer Raman spectra under 676.4-nm excitation (see Sec. III B). The underlying mechanism is probably combined trapping of a released $M^0(1)$ electron and an anion vacancy by two next-nearest-neighbor (NNN) M^+ ions. The same OT3 bleach, performed at 260 K, yields only a very small bleaching effect.

In RbCl:Ga^+ and RbCl:In^+ x-ray irradiation above 260 K leads to the presence of an intense dimer spectrum (Fig. 3), observable under 676.4-, 647.1-, and 632.8-nm excitation. Neither the Raman spectra nor the optical-absorption data allow one to draw definite conclusions about the presence of $Ga^0(1)$ and $In^0(1)$ defects. Superposition of a large number of low-frequency Raman modes prohibits the identification of the $M^0(1)$ centers without additional knowledge on the position of the absorption bands.

B. Raman spectra and optical absorption

The identification of the $Ga^+Ga^0(1)$ and $In^+In^0(1)$ dimer centers is based on the resemblance of the Raman spectra to those, previously detected under OT3 excitation, of $Tl^+Tl^0(1)$.[14] The spectra of Figs. 2 and 3 exhibit the same, completely polarized spectral features, which are not detected in x-ray-irradiated pure KCl and RbCl. No low-frequency mode is correlated with this broadband spectrum, which makes this phenomenon a characteristic feature of the $M^+M^0(1)$ defect.[14] The sharp resonance at about 115 cm^{-1} in the RbCl spectra (Fig. 3) shows at least two overtones for $Ga^+Ga^0(1)$ and one for In^+ $In^0(1)$, analogous with the observations for $Tl^+Tl^0(1)$.[14]

In optical absorption the OT3 bleach of the $Ga^0(1)$ and $In^0(1)$ defects (see Sec. III A) uncovers two underlying absorption bands at 630 and 660 nm, as is shown in Fig. 4 for KCl:Ga^+. The parallel behavior of the optical densities and the Raman intensities permits the association of the 660-nm band with the dimer centers. As such the OT3's of the Ga and In dimer centers in KCl show a red shift relative to those of $Ga^0(1)$ and $In^0(1)$ (605 and 610 nm, respectively), comparable with the ODMR results for the Tl centers in KCl [OT3 of $Tl^0(1)$ at 550 nm and $Tl^+Tl^0(1)$ at 635 nm]. ODMR measurements would be helpful in testing these assignments and for further unraveling the Raman spectra of Ga^+- and In^+-doped RbCl.

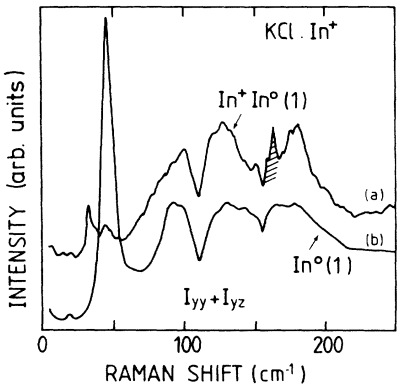

FIG. 6. Resonant Raman spectra of the $In^+In^0(1)$ and $In^0(1)$ defects in KCl. Production procedures are mentioned in the captions of Figs. 2(b) and 5(b), respectively. The shaded area in the dimer spectrum is discussed in Sec. IV C 3.

IV. DISCUSSION

A. Resemblance of the $M^+M^0(1)$ and $M^0(1)$ spectra

The resonant Raman spectra of the $Tl^0(1)$, $In^0(1)$, and $Ga^0(1)$ defects in KCl under OT3 excitation (see Fig. 5) are completely polarized and consist of a broadband spectrum and a low-frequency mode due to the M^0 vibration along the fourfold axis. In Fig. 6 the resemblance in the spectral composition of the $M^0(1)$ and the $M^+M^0(1)$ broadband spectrum is demonstrated. The localized mode dominates the $M^0(1)$ spectra, especially in the case of $Tl^0(1)$, and this has obscured the similarity between $M^+M^0(1)$ and $M^0(1)$ broadband spectra in $KCl:Tl^+$.[14]

The broadband spectrum is excited in a frequency range overlapping the OT3's of both the $M^0(1)$ and $M^+M^0(1)$ centers. We established that two separate absorption bands of two different defects are involved [605 nm for $Ga^0(1)$, 660 nm for $Ga^+Ga^0(1)$] by suitable optical treatment of the $Ga^0(1)$ defects in KCl: The broadband spectrum was detected under 676.4, 647.1-, and 568.2-nm excitation. In contrast, the low-frequency $Ga^0(1)$ mode at 59 cm^{-1} only occurs under 647.1- and 568.2-nm excitation. The OT3 bleach of the $Ga^0(1)$ centers, performed with an interference filter at 600 nm (Sec. III A), enhances the Raman intensity of the 676.4-nm spectrum, strongly reduces the intensity of the low-frequency mode under 647.1-nm excitation [compare Figs. 2(a) and 5(a)], and conserves a relatively intense broadband contribution. The localized mode and the broadband spectrum in the 568.2-nm spectrum [this spectrum is before OT3 bleach similar to that of Fig. 5(a)] disappear *simultaneously*, proving that a preferential $M^0(1)$ bleaching occurs.

The similarity between $M^0(1)$ and $M^+M^0(1)$ Raman characteristics in $RbCl:M^+$ was not systematically investigated. The Raman spectrum of the $Tl^0(1)$ defect in RbCl under 597-nm excitation, presented in Ref. 13, shows the same 117-cm^{-1} resonance as detected for the dimer spectrum of Fig. 3(c). However, the 597-nm excitation wavelength is far from resonance with the $Tl^+Tl^0(1)$ OT3 maximum at 665 nm, and therefore this peak is probably a characteristic Raman feature for both defects. In $RbCl:In^+$ the dimer spectrum with the characteristic 116-cm^{-1} mode [see Fig. 3(b)] is observed under 676.4-nm excitation after x-ray irradiation at 260 and 300 K. The 568.2-nm Raman spectra, on the contrary, contain the 116-cm^{-1} peak only after x-ray irradiation at 260 K. This defect, characterized by similar Raman features as the $In^+In^0(1)$, but with different production properties, may well be the $In^0(1)$ center.

B. BT analysis of the Raman spectra

In the behavior-type (BT) analysis of the OT3 resonant Raman data for the $Tl^+Tl^0(1)$ centers it was shown that the complete polarization of the spectra allows the application of the BT method for nonresonant Raman scattering.[13,14] The intensity parameter ratios $s/q=0$ and $r/q=0$, derived from the polarized Raman intensities, correspond to an observed BT50, which identifies the modes as $C_{4v}:A_1$ modes.[16]

The question is asked whether these observations are consistent with the hopping model for the $Tl^+Tl^0(1)$, outlined in the Introduction. It was mentioned that the symmetry, observed for the dimer defect, depends on the time scale of the experimental (EPR or optical) probe. The resemblance between dimer and monomer spectra (see Fig. 6) shows that Raman excitation frequencies of about 10^{15} Hz probe the instantaneous configuration of the dimer, i.e., that of a static, perturbed $Tl^0(1)$ center with C_{1h} symmetry. Moreover, the spectral composition of the dimer Raman data in KCl hardly differs from that of the unperturbed $M^0(1)$ (see Sec. IV A), apart from the absence of a low-frequency mode. Also the polarization properties, which can be expected to be sensitive to a deviation from the pure C_{4v} symmetry, are not changed. In a completely analogous way as for the $Tl^0(1)$ defect, selective resonant enhancement of one diagonal Raman tensor element[13] due to the strong σ polarization of the OT3, obscures the actual BT and the 12° tilting of the p orbital with respect to the [100] direction is not detected. A similar case, in which the resonant Raman data yield a higher symmetry than the actual one, is the off-center $F_A(Li^+)$ center in KCl under F_{A_1} excitation.[19]

In Ref. 14 the BT analysis of the $Tl^+Tl^0(1)$ spectra was shown to be compatible with both $C_{2v}:A_1$ and $C_{1h}:A'$ modes. It was suggested that, under the assumption of a linear coupling between the phonons and the electron tunneling, the modes in the dimer spectrum could be either $C_{2v}:A_1$ modes or combination modes of $C_{2v}:B_1$ vibrations and $C_{2v}:B_1$ tunneling transitions. The observation of the C_{1h} symmetry of the dimer, discussed above, has its consequences for the distinction made in Ref. 14: both $C_{2v}:A_1$ and $C_{2v}:B_1$ modes reduce to $C_{1h}:A'$ modes.

C. Nonatomic behavior of the $M^0(1)$ defect in its third excited state

1. *Impurity-induced first-order spectra*

Pure alkali halides do not exhibit first-order Raman scattering. The introduction of an impurity into the lattice breaks down the inversion symmetry except at the impurity and, consequently, impurity-induced first-order scattering becomes allowed. The Raman-active modes do not involve defect motion and are therefore independent of the impurity mass. The shape and intensity of the observed spectrum are determined by the force constants in

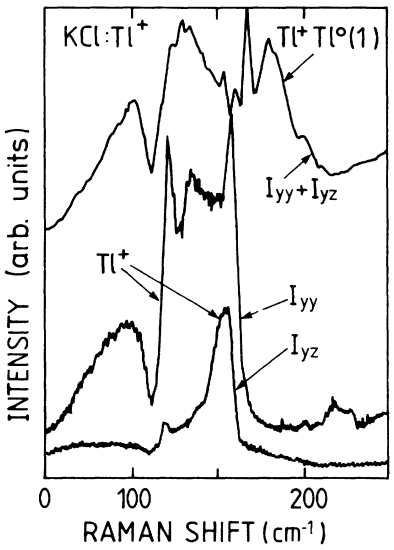

FIG. 7. Tl^+-induced first-order spectrum in KCl. The I_{yy} (a) and I_{yz} (b) spectra were excited with 600 mW of the 514.5-nm line of the Ar^+ laser. Spectrum (c) shows the $Tl^+Tl^0(1)$ spectrum in KCl (see also Fig. 2).

the perturbed crystal. In order to facilitate the discussion of the dimer spectra, the Tl^+-induced Raman spectra for KCl and RbCl are presented in Figs. 7 and 8.

2. *Spectral composition of the dimer spectra*

Despite the resonant enhancement, which determines the polarization properties, and the different defect structure the dimer spectrum and the Tl^+-induced spectrum show striking similarities, which are most prominent for RbCl (Figs. 3 and 8). Also in KCl (Fig. 7) the acoustic region up to 100 cm^{-1} is very similar and apart from the two sharp peaks at 122 and 159 cm^{-1} in the induced spectrum, an increased phonon density between 100 and 155 cm^{-1} occurs for both the dimer and the isolated Tl^+ defect. Larger deviations are found in the optical phonon region above 165 cm^{-1}. In this region the F center is known to exhibit strong resonant Raman scattering, in particular under K-band excitation.[18]

Resonant Raman scattering is a sensitive technique to study the electron-phonon coupling.[20] Surprisingly, the phonons broadening the OT3 of the $M^0(1)$ centers are also present in the projected density of states of the M^+-perturbed lattice.

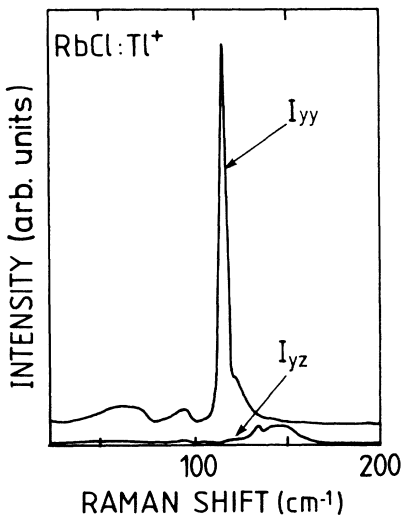

FIG. 8. Tl^+-induced first-order spectrum in RbCl. The I_{yy} (a) and I_{yz} (b) spectra were excited with 300 mW of the 514.5-nm line of the Ar^+ laser.

3. *Comparison with calculated Tl^+-induced Raman spectra*

It is instructive to consider the experimental and theoretical study on defect-induced off-resonance Raman scattering in Tl^+-doped alkali halides by Harley, Page, and Walker,[17] which was extended by Robbins and Page.[21] In Ref. 20 the E_g and T_{2g} contributions of the Tl^+-induced spectra in KCl and RbCl were calculated in the harmonic approximation, using unperturbed (breathing) shell model phonons in a Lifschitz Green's-function formalism. The assumption was made that the electron-phonon interaction is linear in the displacements of the impurity's nearest neighbors (NN). The A_{1g} spectra were not interpreted because of their relatively low experimental accuracy. The best fit of the experimental data for the E_g spectra in $KCl:Tl^+$ was obtained by a 10% stiffening of the impurity NN force constants compared to the force constant k of the pure lattice. For $RbCl:Tl^+$ a 10% weakening gave the most satisfactory results. In addition a complete set of E_g spectra was presented for $KCl:Tl^+$ (Figs. 11 and 12 of Ref. 20) for relative force-constant changes $\delta k/k$ between 0.2 and -0.2, showing the tendency that for stiffening force constants the sharp 122-cm^{-1} feature of Fig. 7 loses its pronounced character compared to the phonon density between 125 and 150 cm^{-1}. As such the dimer system turns out to be an experimental demonstration of the calculated strong force-constant-stiffening case.

It is also worth mentioning that the calculations of Ref. 17 did not predict the strong peak at 159 cm^{-1}, visible in the I_{yy} spectrum of Fig. 7. The inclusion of both NN and NNN displacements in the electron-phonon interaction was shown to improve the agreement between theory and experiment significantly.[21] This leads to an interesting consideration for more subtle differences between the dimer and monomer spectra: The 165-cm^{-1} resonance in the KCl:dimer spectra (shaded area in Fig. 6) is completely absent in the $M^0(1)$ spectra, eliminating the explanation of resonant enhancement of the 159-cm^{-1} mode of the pure first-order spectrum (Fig. 7). The importance of NNN displacements for the phonon density in this region of the Raman spectrum, established in Ref. 21, indicates the possibility that this resonance reflects the perturbation by the second-NN M^+ nucleus.

4. *The F-center character of the Σ state: $F_A(M^+)$ versus $M^0(1)$*

The presence of M^+-like features in the OT3 Raman spectra of the $M^0(1)$ defect indicates a delocalization of the electron density of the third excited state into the anion vacancy. The enhanced Raman scattering intensity above 165 cm^{-1}, which is seen in the dimer spectrum and not in the M^+-induced spectrum, is also considered to be due to this delocalization.

The four-parameter atomic model for the $M^0(1)$ center[3,22] provides remarkably good fits for the absorption band energies and the polarization properties of OT1 and OT2. This is surprising, since a comparison of the experimental **g**- and **A**-tensor value of the $M^0(1)$ ground state with the corresponding free electron values yields an electron delocalization of 45%.[1] For the ground state of the pure F center more than 97% of the electron density is localized in the vacancy.[23] Therefore, the F-center-like features, observed in the OT3 Raman data, indicate that an adequate description of the Σ state within the atomic model is very improbable, and that a description with mixed Tl^0-F_A(Tl) wave functions might be more appropriate.[11] This was not sufficiently emphasized in earlier investigations of the Σ state of $Tl^0(1)$.

First, the Mollwo-Ivey relation of the F center,[23] connecting the absorption band energies with the lattice parameter, also holds for the third optical band of $Tl^0(1)$.[24,25] Second, in the magneto-optical studies the MCD cross section under OT3 excitation for centers, oriented perpendicularly to the magnetic field, calculated within the framework of the atomic model, does not agree in size and sign with the experimentally observed values.[4,10,11] However, the negative MCD sign, predicted by similar calculations for the equivalent p-s transition of the $Tl^0(2)$ defect (i.e., a Tl^0 ion with two anion vacancies along the fourfold axis) in KCl, was confirmed by the experimental data.[11] Apparently, the symmetrical form of the potential is correlated with a larger electron density on the Tl nucleus. Third, the laser-induced reorientation of the $Tl^0(1)$,[24] $In^0(1)$, and $Ga^0(1)$ defects under OT3 excitation,[26] which does not occur under OT1 and OT2 excitation,[24] has no explanation within the atomic model.

The OT3 of the $Tl^0(1)$ defect in NaCl does not completely coincide with the F band.[25] It was argued previously that the size mismatch of the Tl^+ ion in the NaCl lattice yields a strong relaxation of the Tl^0 atom towards the anion vacancy, which alters the transition energies and the EPR hyperfine parameters.[11] This relaxation results in a more symmetric charge distribution and suppresses the F-center character. The absence of a broadband contribution in the Raman spectrum of $Tl^0(1)$ in NaCl is consistent with this observation.[13,15]

D. Absence of low-frequency mode in dimer spectra

The systematic absence of a low-frequency mode in the dimer spectra for all host lattices and doping impurities is at first sight not consistent with the model of a slightly perturbed $M^0(1)$ defect (Sec. I). The hopping of the unpaired electron between the two $M^0(1)$-like p orbitals reduces the coupling of the M^0-vibration with the third optical transition. Broadening of electronic transitions by phonons is caused by changes in overlap between the electronic wave functions involved, due to the modulation of the potential by the phonons. When the frequency of the moving electron is comparatively large or even larger than the characteristic M^+-vibrational frequency, the modulation of the potential is reduced and so is the change in overlap. Consequently, no low-frequency M^+ mode is detected in the Raman spectrum.

Other dynamical systems, also exhibiting two simultaneous motions with different frequencies, are the superionic conductors α-AgI and α-$RbAg_4I_5$, the basic dynamics of which involve nonlocal ionic hopping or diffusion (cf. the electron motion in the dimer center) and localized oscillation of the ion at one particular site (cf. the M^+ vibration in the dimer). The Raman spectrum of α-AgI at 523 K shows strong quasielastic scattering and no low-frequency mode.[27] The hopping or diffusion frequency and the oscillation frequency of the Ag^+ ion in its potential well prior to hopping are found to be 13.3 and 17 cm^{-1}, respectively. In contrast, in the Raman data of α-$RbAg_4I_5$ at 360 K, apart from the quasielastic scattering, also a 20-cm^{-1} mode is detected:[28] The hopping frequency is estimated to be 2.3 cm^{-1}, which is only about 10% of the vibrational frequency.[28,29]

The continuous diffusion model[30] describes the continuous motion of the mobile ion between periodic potential minima, separated by barriers of height A. For a periodic modulation of the polarizability the scattering intensity yields both an inelastic vibrational mode and a quasielastic contribution, when the ion is well localized in the potential well (small k_BT/A). For larger values of k_bT/A, corresponding to a decreased localization of the mobile ion, both Raman lines broaden, the vibrational peak shifts to lower frequencies and finally merges in the quasielastic line: The Raman response of the oscillatory motion strongly depends on the degree of localization of the mobile ion.[31]

Analogously, the nonobservability of the low-frequency mode in the dimer spectrum can be considered as a case of extreme Raman line broadening due to the small localization of the electron on one single Tl^+ nucleus. The hopping frequency is estimated to be at least 30 cm^{-1}. The nonadiabaticity of the electron motion has important implications for the Raman response of the dimer center.

E. Resonant Raman scattering under OT4 excitation

A correct assignment of resonant Raman spectra cannot be made without detailed knowledge on the absorption band energies of the defect under study. Therefore caution should be taken about the interpretation of the Raman spectra excited in the fourth optical transition of the $Tl^+Tl^0(1)$ performed in Ref. 14. With the help of the tagged MCD data for $Tl^+Tl^0(1)$ in KCl, showing a rather broad band centered at 450 nm with substructure on both the high- and low-frequency sides,[12] OT4 Raman spectra were recorded under 457.9-nm excitation: no resemblance with the OT3 spectra was detected. On the other hand, in KBr and RbCl, the Raman data under 514.5-nm excitation were similar to the OT3 spectra. The

discrepancy in OT3-OT4 resemblance, depending on the host lattices, is a subject for further investigation. Apart from the spectral similarity of the OT3 and OT4 data in KBr and RbCl, a clear depolarization was observed under OT4 excitation in both crystals, revealing the actual C_{1h} symmetry and thus the tiling of the p orbital. Moreover, a low-frequency mode occurs in these OT4 spectra, at variance with the OT3 spectra.

This complex situation stimulated us further to investigate the Ga^+- and In^+-doped alkali halides for a possible relation between OT3 and OT4 Raman data. In KCl the spectra under 406-nm excitation show a strong resemblance with the OT3 data, i.e., zero I_{yz} intensity and no low-frequency mode present. In RbCl:In^+ under 568.2–514.5-nm excitation a strong 110.5-cm^{-1} mode can be considered as the OT4 counterpart of the 116-cm^{-1} mode under OT3 excitation, analogous with the 117-cm^{-1} (OT3) and 112-cm^{-1} modes (OT4) of $Tl^+Tl^0(1)$ in RbCl.[14] However, for different x-ray irradiation and optical treatments of the RbCl:In^+ samples, no intensity scaling is found between these candidate-OT4 spectra and the OT3 spectra of Fig. 3. It is still possible that both in RbCl:Tl^+ and RbCl:In^+ a defect is present, different from the dimer, but with similar Raman characteristics in the 110-cm^{-1} region.

An extensive Raman investigation is predominantly hampered by (i) the absence of laser lines between 454 and 406 nm and by (ii) the large number of unknown radiation defects, evidenced by both the complicated optical-absorption and Raman data. Accurate ODMR measurements would clarify the Raman investigations considerably by discerning between the OT3 and OT4 excitation regions of dimer and monomer.

V. CONCLUDING REMARKS

Resonant Raman measurements were performed in x-ray-irradiated RbCl containing the heavy-metal impurities Ga^+ and In^+, while the earlier Raman data for KCl, doped with Ga^+ and In^+,[13,14] were further elaborated. A combined analysis using (a) existing EPR and ODMR data on Tl^+-doped samples, (b) the mutual resemblance of the Raman spectra, and (c) specific features in the optical-absorption data, allow one to identify the isoelectronic $Ga^+Ga^0(1)$ and $In^+In^0(1)$ defects in KCl and RbCl.

The $M^+M^0(1)$ and $M^0(1)$ defects exhibit, in addition to their similar optical-absorption and emission properties, a strong resemblance in production properties and spectral composition of the resonant Raman spectra. These observations are consistent with the hopping model, assuming the unpaired electron hopping between two slightly perturbed $M^0(1)$-like configurations. The observed BT is deduced from the polarized Raman intensities and corresponds to a higher symmetry than the actual one. The resemblance with the monomer spectra allows one to identify the Raman modes in the dimer spectrum as totally symmetric C_{1h}:A' phonons, coupling to the third optical transition, which is strongly σ polarized.

The striking resemblance between the resonant Raman spectra of the $M^0(1)$-like defects and the M^+-induced first-order spectrum, indicates a larger electron density in the anion vacancy for the third excited state. This more pronounced F-center character of the $M^0(1)$ defect in its Σ state was previously suggested by various experiments.

The dimer Raman spectra do not exhibit a low-frequency mode of the heavy-metal ion, in contrast with the monomer spectra. The nonadiabacity of the hopping motion of the unpaired electron determines the Raman response of the M^0 vibrational mode.

The overall consistency of the resonant Raman data under excitation of the third optical transition of the $M^0(1)$-like defects in KCl and RbCl allows a detailed analysis of the structral, dynamical, and electronic properties of these defects, in particular the F-like behavior in the third excited state. A reliable extension to higher excited states is not possible without any further knowledge on their transition energies.

ACKNOWLEDGMENTS

We thank W. Gellermann for supplying many of the samples. This work was supported by NFWO (Nationaal Fonds voor Wetenschappelijk Onderzoek) and IIKW (Interuniversitair Instituut voor Kernwetenschappen), to which the authors are greatly indebted. We also thank A. Bouwen for excellent experimental support.

*Present address: Natuurkundig Laboratorium, Universiteit van Amsterdam, Valakenierstraat 65, 1018 XE Amsterdam, The Netherlands.

[1]E. Goovaerts, J. Andriessen, S. V. Nistor, and D. Schoemaker, Phys. Rev. B **24**, 29 (1981).

[2]P. G. Baranov and V. A. Khrantsov, Phys. Status Solidi B **101**, 153 (1980).

[3]L. F. Mollenauer, N. D. Vieira, and L. Szeto, Phys. Rev. B **27**, 5332 (1983).

[4]F. J. Ahlers, F. Lohse, J.-M. Spaeth, and L. F. Mollenauer, Phys. Rev. B **28**, 1249 (1983).

[5]W. Gellermann, F. Lüty, and C. R. Pollock, Opt. Commun. **39**, 391 (1981).

[6]L. F. Mollenauer, N. D. Vieira, and L. Szeto, Opt. Lett. **9**, 414 (1982).

[7]S. V. Nistor, E. Goovaerts, A. Bouwen, and D. Schoemaker, Phys. Rev. B **27**, 5797 (1983).

[8]S. V. Nistor, I. Heynderickx, E. Goovaerts, and D. Schoemaker, Phys. Status Solidi B **130**, 175 (1985).

[9]W. Van Puymbroeck, J. Andriessen, and D. Schoemaker, Phys. Rev. B **24**, 2412 (1981).

[10]F. J. Ahlers, F. Lohse, Th. Hangleiter, J.-M. Spaeth, and R. H. Bartram, J. Phys. C **17**, 4877 (1984).

[11]F. H. Ahlers, Ph.D. thesis, University of Paderborn, 1985.

[12]F. J. Ahlers, F. Lohse, and J.-M. Spaeth, J. Phys. C **18**, 3881 (1985).

[13]W. Joosen, E. Goovaerts, and D. Schoemaker, Phys. Rev. B **32**, 6748 (1985).

[14]W. Joosen, E. Goovaerts, and D. Schoemaker, Phys. Rev. B **35**, 8215 (1987).

[15]W. Joosen, C. Sierens, and D. Schoemaker, Solid State Commun. **63**, 69 (1987).

[16]J. F. Zhou, E. Goovaerts, and D Schoemaker, Phys. Rev. B **29**, 5509 (1984).
[17]R. T. Harley, J. B. Page, and C. T. Walker, Phys. Rev. B **3**, 1365 (1971).
[18]D. S. Pan and F. Lüty, in *Proceedings of the Third International Conference on Light Scattering in Solids, Campinas, Brazil,* 1975, edited by M. Balkanski, R. C. C. Leito, and S. P. S. Porto (Flammarion, Paris, 1975), p. 539.
[19]M. Leblans, W. Joosen, E. Goovaerts, and D. Schoemaker, Phys. Rev. B **35**. 2405 (1987).
[20]C. H. Henry and C. P. Slichter, in *Physics of Color Centers,* edited by W. B. Fowler (Academic, New York, 1968).
[21]D. Robbins and J. B. Page, Phys. Rev. B **13**, 3604 (1976).
[22]N. D. Vieira, L. F. Mollenauer, and L. H. Szeto, Solid State Commun. **50**, 1037 (1984).
[23]W. B. Fowler, in *Physics of Color Centers,* edited by W. B. Fowler (Academic, New York, 1968).
[24]W. Gellermann, T. Jock, and F. Lüty (unpublished).
[25]M. Fockele, F. J. Ahlers, F. Lohse, J.-M. Spaeth, and R. H. Bartram, J. Phys. C **18**, 1963 (1985).
[26]C. Sierens, W. Joosen, and D. Schoemaker, Phys. Rev. B **37**, 3075 (1988).
[27]M. J. Delaney and S. Ushioda, in *Physics of Superionic Conductors,* edited by M. B. Salamon (Springer, Berlin, 1979).
[28]D. A. Gallagher and M. V. Klein, Phys. Rev. B **19**, 4282 (1979).
[29]R. A. Field, D. A. Gallagher, and M. V. Klein, Phys. Rev. B **18**, 2995 (1978).
[30]T. Geisel, *Physics of Superionic Conductors,* edited by M. B. Salamon (Springer, Berlin, 1979).
[31]T. Geisel, Solid State Commun. **24**, 155 (1977).